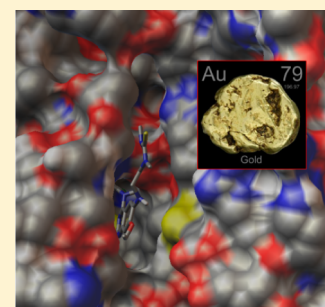


Synthesis, Reactivity, and Biological Activity of Gold(I) Complexes Modified with Thiourea-Functionalized Tyrosine Kinase Inhibitors

Mu Yang,[†] Amanda J. Pickard,[†] Xin Qiao,[‡] Matthew J. Gueble,[†] Cynthia S. Day,[†] Gregory L. Kucera,[§] and Ulrich Bierbach^{*,†}[†]Department of Chemistry, Wake Forest University, Winston-Salem, North Carolina 27109, United States[‡]School of Pharmaceutical Sciences, Tianjin Medical University, Tianjin 300070, PR China[§]Department of Internal Medicine, Hematology–Oncology Section, Wake Forest University Health Sciences, Winston-Salem, North Carolina 27157, United States

S Supporting Information

ABSTRACT: Thiourea-modified 3-chloro-4-fluoroanilino-quinazoline derivatives have been studied as potential receptor-targeted carrier ligands in linear gold(I) complexes. The molecules mimic the epidermal growth factor receptor (EGFR) tyrosine kinase-targeted inhibitor gefitinib. Thiourea groups were either directly attached to quinazoline-C6 (compounds 4, 5, and 7) or linked to this position via a flexible ethylamino chain (compound 9). Compound 7 acts as a thiourea-S/quinazoline-N1 mixed-donor ligand, giving the unexpected dinuclear complex $[\{Au(\mu-7-S,N)\}_2]X_2$ ($X = Cl^-, SCN^-$) (12a,b) (X-ray crystallography, electrospray mass spectrometry). Derivative 9 forms a stable linear complex, $[Au(PEt_3)(9-S)](NO_3)$ (13). The biological activity of the carrier ligands and corresponding gold(I) complexes was studied in NCI-H460 and NCI-H1975 lung cancer cells. Compound 9 partially overcomes resistance to gefitinib in NCI-H1975, a lung cancer cell line characterized by a L858R/T790M mutation in EGFR (IC_{50} values of 1.7 and 30 μM , respectively). The corresponding gold complex (13) maintains activity in the low-micromolar concentration range similar to the metal-free carrier. Compound 9 and the corresponding $[Au(PEt_3)]$ complex, 13, inhibit EGFR kinase-mediated phosphorylation with sub-micromolar IC_{50} values similar to those observed for gefitinib under the same assay conditions. Potential mechanisms of action and reactions in biological media of this new type of hybrid agent, as well as shortcomings of the current design are discussed.



■ INTRODUCTION

Gold(I)-based complexes display a wide range of biological activities, which are thought to be mediated by the metal's reactions with (seleno)cysteine residues in proteolytic and redox-active enzymes, in particular, thioredoxin reductase (TrxR).¹ While these interactions are often nonspecific due to relatively fast ligand exchange rates, fortuitous targeting of specific cysteine residues by gold(I) complexes containing sufficiently long-lived carrier ligands has also been reported.² Several new lines of research suggest that gold(I) has a significant potential as a component of therapies designed to inhibit therapeutically relevant targets, such as zinc-finger domains³ and protein kinases.⁴

We were interested in the possibility of introducing reactive gold(I)-based electrophilic groups into inhibitors of tyrosine kinase (TKIs) with the goal of hijacking a thiophilic metal into the active site of this therapeutically important enzyme.⁵ One potential binding mechanism of these agents with epidermal growth factor receptor tyrosine kinase (EGFR-TK) would involve reaction of gold(I) with the solvent-accessible cysteine thiol residue (Cys-797) near the entrance to the enzyme's binding pocket.⁶ Such a mechanism might potentially inhibit binding of ATP and, consequently, kinase-mediated phosphorylation more effectively than reversible binding of the TKI

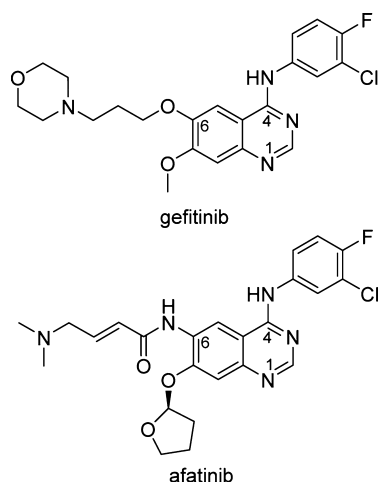
alone. The desired pharmacophore would combine the high sulfur affinity of gold(I) with the selectivity and submicromolar binding affinity of an EGFR-TK-targeted ligand.

Mutationally activated EGFR-TKs are considered a major driver of cancer cell survival and aggressive tumor growth.⁵ In nonsmall cell lung cancer (NSCLC), expression levels of EGFR are inversely correlated with survival of the disease.^{7,8} Somatic (activating) EGFR mutations sensitize cancer cells to small-molecule TKIs, which target the enzyme's ATP binding site and show potent antiproliferative properties.⁹ Gefitinib (Chart 1) is a quinazoline-based TKI indicated against cancers harboring aberrant EGFR, in particular, lung carcinomas.⁹ Unfortunately, the efficacy of this drug is limited by the emergence of acquired resistance as a consequence of a secondary mutation within the ATP binding pocket (T790M).¹⁰ One currently pursued approach to combatting this form of resistance observed for mutant EGFR and other clinically relevant kinases is to turn the reversible TKIs into irreversible inhibitors, such as the recently FDA-approved inhibitor afatinib (Chart 1).¹¹ These molecules contain strategically positioned reactive electrophilic groups (usually Michael acceptors), which are able to form a covalent

Received: December 17, 2014

Published: March 20, 2015



Chart 1. Structures of Gefitinib and Afatinib Showing Relevant Atom Numbering for the Quinazoline Scaffold

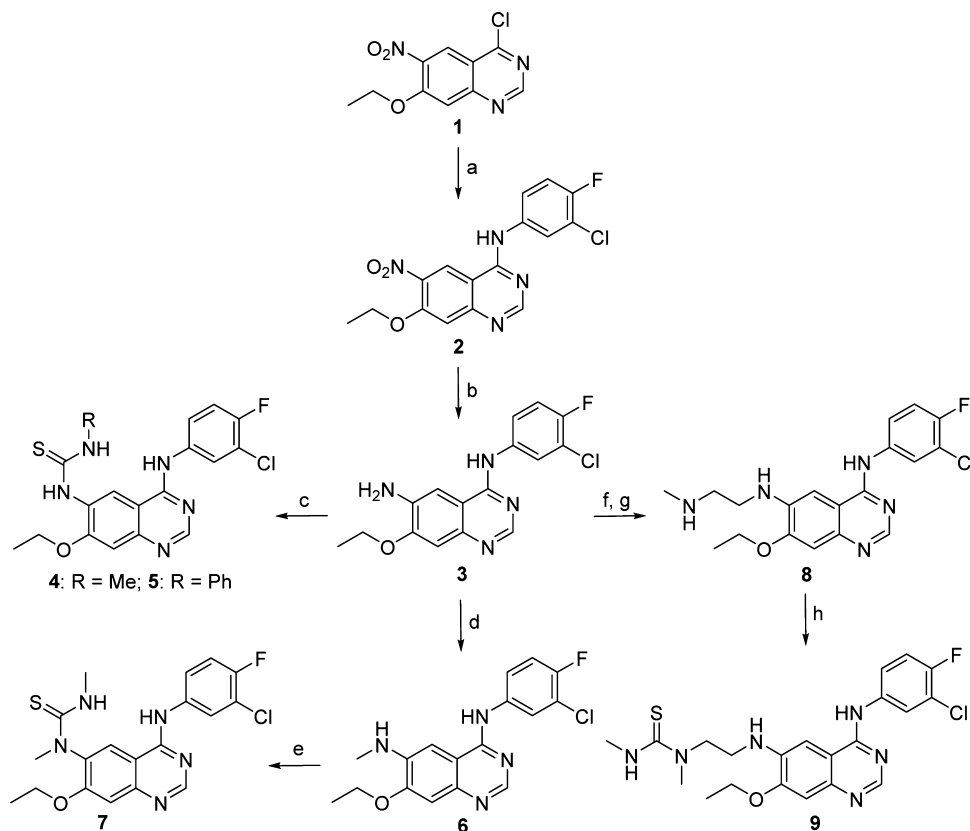
bond with accessible cysteine residues in the active sites of targetable enzymes. Several irreversible TKIs are currently being evaluated in the clinic.¹²

Introduction of gold(I) as a cysteine-targeting moiety in place of a Michael acceptor can be considered a new strategy of improving the activity of TKIs against resistant disease. The purpose of the current study was to assess if the gefitinib-type quinazoline scaffold can be functionalized with a thiourea

moiety without compromising the binding affinity of the TKI, and if the S-donor group can be modified with thiophilic (pseudo)halide and phosphine substituted gold(I) electrophiles. A new TKI derivative was identified that strongly binds to the tyrosine kinase ATP-binding pocket and partially overcomes resistance to gefitinib in NSCLC cell lines harboring wild-type and mutated EGFR kinase domains. In the corresponding gold(I) complex, the metal appears to have an effect on both the biological activity and kinase binding affinity of the inhibitor, but the linear thiourea–Au(I)–phosphine coordination appears to be too labile for the desired targeted application.

RESULTS AND DISCUSSION

Synthetic Studies. To generate a gold-modified TKI, we borrowed the N-heterocyclic quinazoline scaffold and the N-(3-chloro-4-fluorophenyl) group from gefitinib (Chart 1), which target the adenine binding site and an adjacent hydrophobic pocket of EGFR-TK, respectively.¹³ The 6-position of the quinazoline C₆ ring was chosen as attachment point for a side chain carrying a cysteine-affinic gold(I) moiety, similar to the design of clinically relevant Michael acceptor-based irreversible TKIs.¹¹ The goal of this design was to favor binding of the metal with cysteine-797 proximal to the kinase's catalytic cleft without compromising the ligand's interactions with the binding pocket. The linkage between the electrophile and the TKI would be achieved via formation of a strong Au(I)–S bond with a thiourea residue, a thiol-like donor group previously

Scheme 1. Synthesis of Quinazoline Derivatives^a

^aReagents and conditions: (a) 3-chloro-4-fluoroaniline, *i*-PrOH, rt, overnight; (b) Fe, AcOH, NaOAc, MeOH, reflux, 3 h; (c) RNCS, EtOH, rt, 3 h; (d) paraformaldehyde, NaOMe, NaBH₄, MeOH, reflux, 4 h; (e) MeNCs, DMAP, EtOH, reflux, 30 h; (f) *tert*-butylmethyl(2-oxoethyl)carbamate, NaCNBH₃, AcOH, MeOH, rt, 2 h; (g) 4 M HCl, reflux, 2 h; (h) MeNCs, EtOH, rt, 1 h.

explored in biologically relevant carrier ligands of this metal.^{14–16}

We performed a docking study to examine the conformational space and receptor binding of thiourea-modified TKIs. Structures of the gold-free ligands were geometry optimized using DFT calculations and studied in complex with the EGFR kinase domain (L858R/T790M mutant) (PDB-ID: 2JIV). In these experiments we identified scaffolds that produce energetically favorable binding geometries in which the thiourea sulfur of the TKI is positioned in close proximity to the sulfur atom of cysteine-797 (see the Supporting Information). This orientation was considered compatible with electrophilic attack of the metal in a corresponding gold(I)-modified TKI on the protein thiol.

From the initial modeling studies, two promising structures, **4** and **5**, emerged (Scheme 1). The two derivatives (and all other derivatives reported) were synthesized from common intermediate **3**, which was generated by installing a 3-chloro-4-fluoroanilino group at the 4-position of the quinazoline ring in precursor **1**¹⁷ and subsequent reduction of the 6-nitro group in **2** to a 6-amino group. Reaction of **3** with the appropriate isothiocyanates¹⁴ afforded the *N,N'*-disubstituted thiourea derivatives **4** and **5**. Attempts to introduce gold(I) electrophiles such as $[\text{AuX}]$ (where $\text{X} = \text{Cl}^-$ or SCN^-) into these structures using the common precursor $[\text{AuX}(\text{tht})]$ (tht = tetrahydrothiophene),¹⁸ however, were unsuccessful (Scheme 2). Electro-spray mass spectra (ES-MS) of these reaction mixtures showed no sign of the desired ligand exchange to produce complexes $[\text{AuX}(\text{4/5})]$, but were consistent with decomposition of **4** and

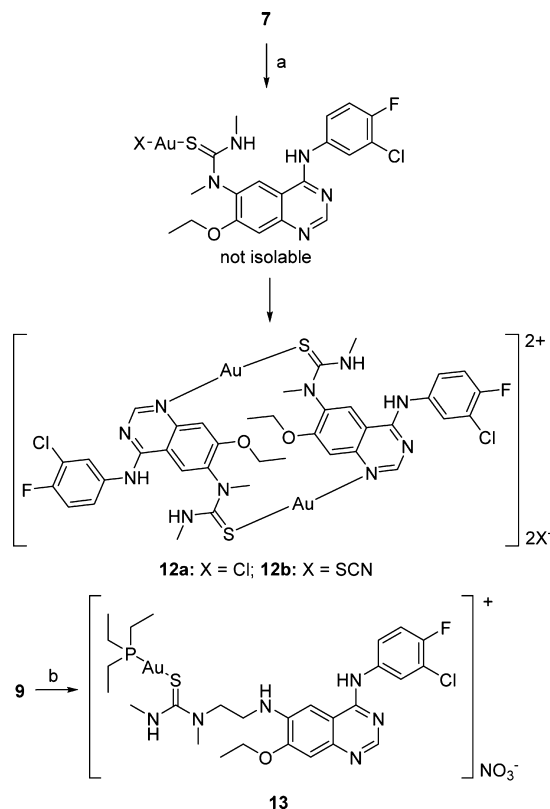
5 resulting in the analogous cyanamides (loss of H_2S , based on $[\text{M} - 34 + \text{H}]^+$ fragment ions, see the Supporting Information) and gold(I) sulfide. Desulfuration of (aromatic) *N,N'*-disubstituted thioureas has previously been observed in the presence of heavy metals.¹⁹

To circumvent the problem of ligand desulfuration, the *N,N,N'*-trisubstituted derivative **7** was synthesized from the *N*°-methylquinazoline derivative **6**, which was generated from intermediate **3** via reductive amination. In reactions with $[\text{AuX}(\text{tht})]$, compound **7** showed greatly improved ligand properties and was able to act a stable sulfur donor. X-ray crystallographic and mass spectrometric analysis of the product isolated from the reaction mixtures indicated that compound **7** does not act as a terminal S-donor ligand in the desired complexes $[\text{AuX}(\text{7})]$. Instead, **7** produces a dinuclear complex, $[\{\text{Au}(\text{7})\}_2]\text{X}_2$, in which **7** acts as a bridging ligand (**12a** and **12b**, Scheme 2). In the solid state structure of **12a**, the Au(I) centers are coordinated by a thiourea-S atom of one ligand and endocyclic quinazoline-*N*¹ of another ligand. This produces an unusual arrangement in which the aromatic moieties of the two bridging ligands are mutually stacked at van der Waals distance (Figure 1a). Proton NMR chemical shift anomalies in conjunction with electrospray mass spectra recorded in positive-ion mode (Figure 1b) confirm that the dinuclear cationic structures persist in solution and are not solely a consequence of packing effects in the solid state. Importantly, no reversal of the dinuclear structure was observed when **12a** was incubated at physiologically relevant concentrations in phosphate-buffered saline for several days (data not shown). This observation suggests that **12a** is not converted back to the corresponding mononuclear complex, $[\text{AuCl}(\text{7})]$, in chloride-rich media.

Attempts to install phosphine as a more inert ligand in place of *X* via reaction of **7** with $[\text{AuCl}(\text{PET}_3)]$ ²⁰ to avoid substitution of the ligand trans to sulfur by quinazoline nitrogen were unsuccessful (no substitution of chloride by thiourea was observed). However, the latter reaction succeeded when the trisubstituted thiourea moiety was incorporated into an extended side chain at the 6-position of the quinazoline scaffold. Introduction of the (2-methylamino)ethyl group involved reductive amination²¹ of **3** to give **8**, which was finally converted to thiourea **9** with isothiocyanate. While compound **9** did not yield the desired gold-modified mononuclear derivative when reacted with $[\text{AuX}(\text{tht})]$, it produced the cationic complex $[\text{Au}(\text{PET}_3)(\text{9})](\text{NO}_3)$ (**13**) (Scheme 2), which proved to be stable with respect to desulfuration and dinucleation (based on ES-MS and NMR data, see the Supporting Information). Characteristic variations in ¹H NMR chemical shifts observed for complex **13** relative to ligand **9** (see Experimental Section) confirm selective binding of the $\{\text{Au}(\text{PET}_3)\}^+$ moiety to thiourea sulfur.

Biological Activity. Cell proliferation assays in two NSCLC cell lines were performed to assess the cell growth inhibitory effects of the newly synthesized TKI derivatives **7** and **9** alone and as ligands in complexes **12a**, **12b**, and **13**. For comparison the clinical drug gefitinib was included in the screening. The cell line NCI-H460 is a model of large-cell lung cancer and is characterized by wild-type EGFR-TK.⁸ By contrast, NCI-H1975 adenocarcinoma cells harbor a point mutation (L858R) in exon 21 as well as a secondary mutation (T790M) at the bottom of the hydrophobic ATP binding pocket.⁸ While the former somatic (activating) mutation

Scheme 2. Synthesis of Gold(I) Complexes^a



^aReagents and conditions: (a) $[\text{AuX}(\text{tht})]$, where $\text{X} = \text{Cl}^-$, **10a**, or $\text{X} = \text{SCN}^-$, **10b**, and tht = tetrahydrothiophene; CH_2Cl_2 , rt, 30 min; (b) $[\text{AuCl}(\text{PET}_3)]$ (**11**), MeOH/THF , AgNO_3 , rt.

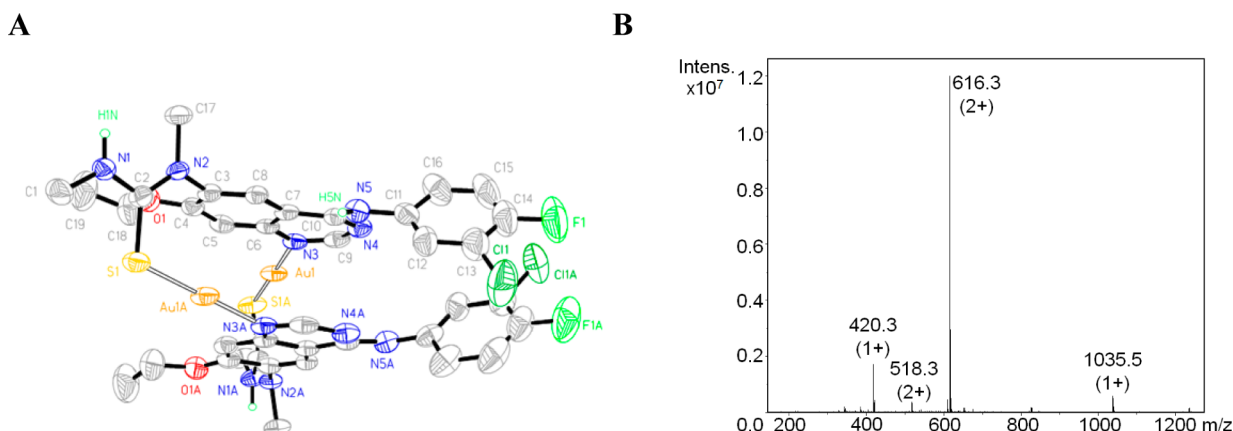


Figure 1. (A) Structure of $[\{\text{Au}(7)\}_2]\text{Cl}_2\cdot\text{DMF}$ (**12a**-DMF) in the solid state with selected atoms labeled. Counterions and crystal solvent have been omitted for clarity. (B) Electrospray mass spectrum recorded in positive-ion mode of dinuclear complex **12a**. Characteristic ions: m/z 420.3 $[\text{7} + \text{H}]^+$, 518.3 $[\text{12a} - \text{Au} + \text{H}]^{2+}$, 616.3 $[\text{12a} - 2\text{Cl}]^{2+}$, 1035.5 $[\text{12a} - \text{Au}]^+$.

sensitizes cancer cells to EGFR-TKIs (including gefitinib), the latter causes resistance to these therapies.⁸

The results of the cell proliferation assays are summarized in Table 1. Both NCI-H460 (wild-type) and NCI-H1975

Table 1. Summary of Cytotoxicity Data (IC_{50} Values)^a

compd	NCI-H460 (EGFR _{wild-type})	NCI-H1975 (EGFR _{L858R/T790M})
7	36.0 ± 4.4	51.7 ± 1.1
9	4.2 ± 0.4	1.7 ± 0.1
12a	19.1 ± 2.0	39.7 ± 1.7
12b	20.1 ± 0.2	31.9 ± 0.4
13	1.9 ± 0.1	2.5 ± 0.1
gefitinib	14.2 ± 0.5	30.0 ± 1.3

^a IC_{50} values \pm SD (μM) were extracted from drug–response curves for two experiments performed in triplicate for each concentration. Cells were incubated for 72 h. The highest concentration of DMF after serial dilution was less than $0.1 \mu\text{M}$.

(mutated) show the expected resistance to gefitinib with inhibitory concentrations in the high micromolar range, in agreement with previously reported data (typically, $\text{IC}_{50} > 10 \mu\text{M}$).³ NCI-H460 cells were found to be more sensitive to all of the analogues tested than NCI-H1975, except for compound **9**. The new analogue **7** was the least active compound tested with high-micromolar IC_{50} values in a range previously observed for structurally related thiourea-modified TKIs.²² By contrast, extension of the side chain on carbon 6 of the quinazoline ring to generate **9** led to a pronounced increase in potency, in particular, in NCI-H1975, where a cytotoxic enhancement of 30-fold is observed. Most notably, compound **9** partially overcomes the acquired resistance against gefitinib observed in this cancer model. The low-micromolar inhibitory concentration determined for compound **9** in *resistant* NCI-H1975 compares favorably with the high-nanomolar/low-micromolar activity typically observed for gefitinib in *sensitive* NSCLC models.⁸ Modification of compounds **7** and **9** with $\{\text{AuX}\}$ and $\{\text{Au}(\text{PET}_3)\}^+$ groups, respectively, had a minor but significant effect on the inhibitory concentrations, with compound **13** maintaining low-micromolar activity in both cell lines. In NCI-H460, complex **13** shows enhanced activity compared to compound **9** by approximately 2-fold.

Compound **9** alone showed significantly better activity than gefitinib in a TKI-resistant cancer cell line. This observation

suggests that the newly introduced thiourea-containing side chain may enhance the binding affinity of the classical TKI structure with the enzyme's active site. In the lowest-energy model generated for compound **9** in complex with EGFR-TK (L858R/T790M mutant) the thiourea-modified side chain is located in the hydrophilic region of the protein cleft produced by the bilobal kinase fold (see the Supporting Information).²³ This orientation positions the thiourea-NH group in close hydrogen-bonding distance to residues Asn-842 and Asp-855, which may promote strong binding to the EGFR-TK domain. Derivative **9** showed promising activity in the cell proliferation assay, but attachment of the gold electrophile in **13** did not result in the desired enhancement in cell kill. One possible explanation for this observation would be that the $[\text{Au}(\text{PET}_3)]^+$ group, while not compromising the binding affinity of the TKI moiety with the receptor, may be positioned unfavorably for reaction with the sulfur atom of cysteine-797. It is also possible that cytotoxic gold–phosphine species, generated from complex **13** by premature intracellular cleavage of the Au(I)–S_{thiourea} bond, may not significantly contribute to the cell kill in the two cancer models, which may be dominated by TK inhibition.

Reactivity of Compound **13** with Cysteine Thiol.

Unlike the initially designed complexes containing Cl^- and SCN^- trans to thiourea sulfur, compound **13** is modified with a strongly trans-labilizing phosphine ligand. We reasoned that this feature should lead to selective cleavage of the Au(I)–S_{thiourea} bond in reactions with competing nucleophiles. One potential consequence of this reactivity would be the transfer of the $[\text{Au}(\text{PET}_3)]^+$ moiety from the EGFR-bound inhibitor **13** to cysteine-797. To study the reactivity of the metal with this target nucleophile, compound **13** was incubated with a cysteine-containing peptide, and the reaction mixture was analyzed by ES-MS. As a model, we chose the sequence QLMPFGCL, which mimics residues 791–798 (including cysteine-797) of the hinge region of EGFR-TK.²⁴ The reaction produces an equilibrium mixture of **9**, $[\text{Au}(\text{PET}_3)]$ –peptide, unmodified peptide, and unreacted complex **13** (Figure 3), confirming that the thiourea and thiolate donors are competing for gold(I) coordination. Thus, the results are in agreement with ligand exchange trans to the phosphine ligand. The mass spectrometric data are also consistent with binding of the $[\text{Au}(\text{PET}_3)]^+$ moiety to the (deprotonated) cysteine-797 residue (Figure 2). The same reactivity was observed when compound

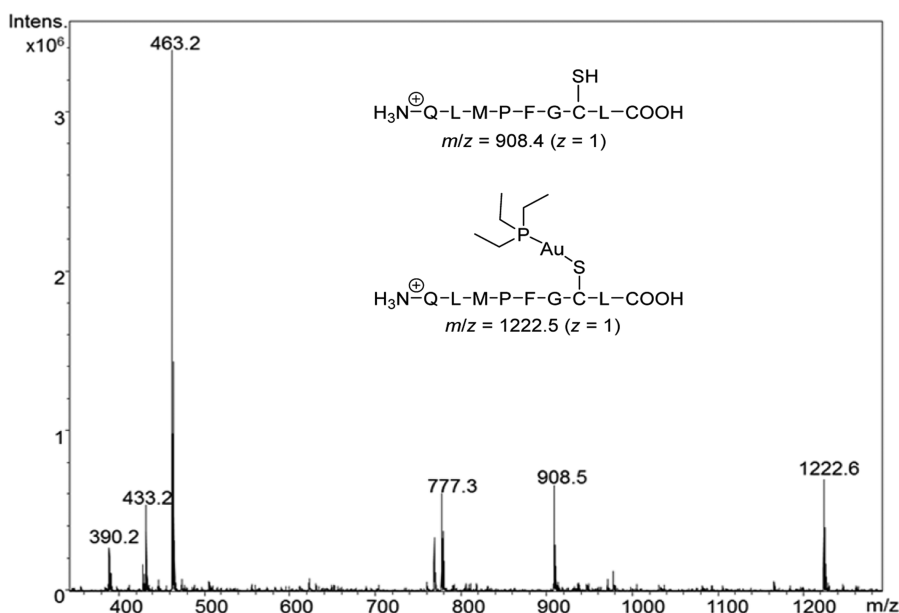


Figure 2. Positive-ion mode electrospray mass spectrum for the reaction of octapeptide QLMPFGCL (50 μ M) with compound **13** (50 μ M) in aqueous phosphate buffer (0.01 M, pH 7.2). Spectra were acquired 30 min after mixing of the solutions and remained unchanged after extended incubation periods. Characteristic ions m/z : 908.5 [QLMPFGCL + H]⁺ (see inset), 1222.6 [QLMPFGCL·Au(PEt₃)₂ – H]⁺ (see inset), 390.2 [13 + H]²⁺, 433.2 [(Et₃P)₂Au]⁺, 463.2 [9 + H]⁺, 777.3 [13]⁺.

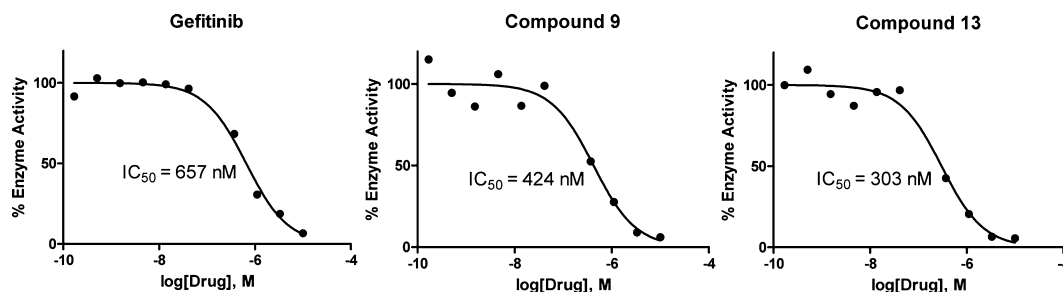


Figure 3. Dose–response curves for titrations of recombinant EGFR_{L858R/T790M} tyrosine kinase with inhibitors. Enzyme activity was determined using an assay that measures conversion of ATP to ADP. Plotted data are averages of two determinations.

13 was reacted with *N*-acetylcysteine and glutathione (data not shown). Thus, cleavage of the Au–S_{thiourea} bond by the latter ubiquitous tripeptide has to be considered an undesired competing mechanism in cells. The thiourea/thiolate ligand exchange reactions occur instantaneously and too rapidly for a comparative kinetic analysis.

Inhibition of EGFR Tyrosine Kinase. Because compounds **9** and **13** contain the 3-chloro-4-fluoroanilino-quinazoline scaffold of gefitinib, our analogues can be expected to act as ATP-competitive inhibitors. To confirm that both compounds are able to inhibit ATP-to-ADP conversion by EGFR-TK (L858R/T790M double mutant) and to test if gold(I) in the latter complex has an effect on kinase activity, we used an assay based on bioluminescent detection of ATP. The assay was performed in a modified buffer free of BSA and DTT to minimize unwanted side reactions of compound **13** with the reactive thiol groups in these molecules. Compounds **9**, **13**, and the clinical drug gefitinib inhibit tyrosine kinase-mediated protein phosphorylation at similar submicromolar levels, which was quantified by monitoring conversion of ATP into ADP (Figure 3). Unlike the covalent inhibitor afatinib, which shows a 100-fold lower IC₅₀ than gefitinib in kinase activity assays performed with EGFR-TK_{L858R/T790M},²⁵ compound **13** did not show the desired enhancement. Although this observation *per*

se does not rule out an irreversible binding mechanism, the instability of compound **13** and the fact that it is not significantly more cytotoxic than gefitinib and compound **9** in NCI-H1975 harboring the EGFR_{L858R/T790M} mutation discouraged us from performing additional experiments to further characterize the mode of inhibition. (For comparison, we also tested the complex [AuCl(PEt₃)₂] (**11**), a potential decomposition product of compound **13** in assay buffer. This compound quenches enzyme activity at much higher micromolar concentrations and does not produce the sigmoidal dose response of **9** and **13**, which would be expected for selective kinase inhibition; see Supporting Information.) The observation that the gold(I) moiety in compound **13** shows no major effect on inhibitory concentrations may indicate a lack of reactivity with the targeted cysteine-797 or loss of the metal in nonspecific reactions with the protein. The results of this assay demonstrate that compound **13** targets the ATP binding pocket of EGFR-TK to produce kinase inhibition similar to gefitinib and compound **9** but does not result in the level of enhancement observed for the Michael-acceptor-based pharmacophores.

CONCLUSIONS

While several peptide and intercalator-containing conjugates have been designed to improve the uptake and organelle selectivity of gold-based cytotoxic agents,^{26–29} introduction of gold(I) moieties as reactive electrophiles into clinically relevant molecularly targeted therapies is an entirely new concept. “Molecularly targeted therapies” are defined as small-molecule inhibitors of aberrant kinase signaling (“nibs”) and monoclonal antibodies targeted at growth receptors (“mabs”).³⁰ The current approach also differs from that pioneered by Meggers et al., which uses rigid, inert transition metal-based scaffolds to target protein kinases.³¹

One potential mechanism of action of compound **13** would involve transfer of the $[\text{Au}(\text{PET}_3)]^+$ moiety to cysteine-797 of the EGFR-TK. While this reaction would not produce a permanent cross-link between the TKI and the enzyme, unlike those observed with the Michael acceptor-modified agents, it would lead to a bulky adduct in the enzyme active site. This form of modification may help block access of ATP to the catalytic pocket to help overcome resistance mediated by the reduced TKI binding affinity in mutated kinase domains. The ability of compound **9** to act as a targeted carrier of $[\text{Au}(\text{PET}_3)]^+$ depends on the stability of the mixed thiourea–phosphine coordination in compound **13** in the presence of competing nucleophiles in circulation and in the cytosol. Thiourea as a donor was chosen for its relative ease of synthesis and for its thiol-like properties and ability to mimic and compete with thiolate sulfur in gold(I) coordination.^{16,32} The results of the mass spectrometry study confirm that thiourea, indeed, is able to compete with thiolate sulfur, but appears to be too labile as a ligand trans to phosphine for the desired targeted application. A major concern of such an entity would be its high reactivity with ubiquitous thiols in circulation and cells (e.g., human serum albumin, glutathione), which would cause systemic instability and undesired off-target effects. Thus, alternative, sterically hindered ligands able to slow ligand exchange remain to be tested as part of a proof-of-concept study and a broader effort to establish structure–activity relationships.

Another (undesired) mechanism by which complex **13** disassembles into a gold–phosphine species and analogue **9** in the presence of reactive bioligands prior to reaching the enzyme active site has also to be considered. Gold(I)–phosphines directly target the mitochondria to trigger oxidative stress, which leads to apoptosis.³³ Aberrant EGFR expression is associated with defective mitochondrial apoptotic signaling, which renders affected cancer cells insensitive to conventional chemotherapy.^{34,35} A dual mechanism promoted by the individual components that involves inhibition of EGFR signaling and cell death triggered by mitochondrial toxicity may help overcome tumor resistance.

In conclusion, using simple ligand substitution chemistry, which has been previously developed to generate mixed thiourea–(pseudo)halido and thiourea–phosphine gold(I) complexes,¹⁴ we were able to introduce a TKI derived from gefitinib as terminal ligand. This was possible after innocuous modification of the cancer drug with a sulfur-donor group. If ligand exchange reactions in these complexes can be controlled more efficiently, such molecules may provide a therapeutically useful strategy for targeting the human kinome with the goal of overcoming tumor resistance to first-line therapies.

EXPERIMENTAL SECTION

General Supplies and Procedures. Hydrogen tetrachloroaurate trihydrate was purchased from Alfa Aesar. The tetrahydrothiophenogold(I) complexes **10a** and **10b**,¹⁸ chlorotriethylphosphinegold(I) **11**,²⁰ compound **1**,¹⁷ and *tert*-butylmethyl(2-oxoethyl)carbamate²¹ were synthesized using published procedures. Gefitinib was purchased from Sigma. For the preparation of biological buffers, biochemical grade chemicals (Fisher/Acros) were used. HPLC-grade solvents were used for all HPLC and mass spectrometry experiments. The synthetic octapeptide, QLMPFGCL, was purchased from Thermo Scientific Pierce Protein Research (Rockford, IL). All other reagents and chemicals were acquired from common vendors and used without further purification. Reactions involving gold were performed and solutions stored in the dark. ¹H NMR spectra of the target compounds and intermediates were recorded on Bruker Advance 300 and DRX-500 instruments. Proton-decoupled ¹³C NMR spectra were recorded on a Bruker DRX-500 instrument operating 125.8 MHz. (Signal multiplicities in peak listings reflect ¹³C–¹⁹F and ¹³C–³¹P coupling. $J(^{13}\text{C}–^{19}\text{F})$ and $J(^{13}\text{C}–^{31}\text{P})$ values are not reported.) Chemical shifts (δ) are reported in parts per million (ppm) relative to tetramethylsilane (TMS).

Electrospray mass spectra (ES-MS) were recorded on an Agilent 1100LC/MSD trap instrument. Ion evaporation was assisted by a flow of N₂ drying gas (300–350 °C) at a pressure of 40–50 psi and a flow rate of 11 L/min. Mass spectra were typically recorded with a capillary voltage of 2800 V over a mass-to-charge (*m/z*) scan range of 200–2200. The purity and stability of the target compounds was analyzed by reverse-phase high-performance liquid chromatography (HPLC) using the LC module of the Agilent Technologies 1100 LC/MSD trap system equipped with a multiwavelength diode-array detector. Separations were accomplished with a 4.6 mm × 150 mm reverse-phase Agilent ZORBAX SB-C18 (5 μm) analytical column at 25 °C. Separations were accomplished with the following solvent system: solvent A—optima water/0.1% formic acid; solvent B—methanol/0.1% formic acid; solvent C—acetonitrile/0.1% formic acid. Separations were performed at a flow rate of 0.5 mL/min and a gradient of 50% A/50% B to 5% A/95% B over 20 min (for **7**), and at a flow rate of 0.5 mL/min and a gradient of 95% A/5% C to 5% A/95% C over 20 min (for **9**). HPLC traces were recorded over a wavelength range of 363–463 nm. Mass spectra of reactions mixtures containing octapeptide and compound **13** were recorded in positive-ion mode for samples directly infused into the electrospray source in 50% solvent A/50% solvent B at a flow rate of 200 $\mu\text{L}/\text{min}$. High-resolution mass spectrometry (HRMS) was performed on a Thermo Scientific LTQ Orbitrap XL equipped with an electrospray source with a capillary voltage of 5000 V over an *m/z* scan range of 200–2200. Samples were introduced into the electrospray source by direct injection utilizing 50% solvent A with 50% solvent B at a flow rate of 100 $\mu\text{L}/\text{min}$. Spectra were recorded in positive-ion mode.

Single crystals of **7** were grown from a saturated solution in methanol, while crystals of **12** were grown by slow diffusion of diethyl ether into a concentrated DMF solution. HPLC peaks were integrated with MestReNova 8.1. For all organic ligands studied in cancer cells, an analytical purity of $\geq 95\%$ was confirmed by reversed-phase HPLC. The purity of compounds **12** and **13** was determined by CHN elemental analysis (Intertek Pharmaceutical Services, Whitehouse, NJ). Single-crystal X-ray data acquired for compounds **7** and **12a** and experimental details of the structure solution and refinement have been deposited with the Cambridge Crystallographic Data Centre (Cambridge, U.K.) under deposition codes CCDC-976611 and CCDC-976612, respectively.

Computational Studies. The inhibitor structures were built in GaussView 4.0 (Semichem Inc., Shawnee Mission, KS, 2009). Structures were optimized at the rb3lyp level of theory using the 6-311** basis set in Gaussian 03 (Gaussian, Inc., Pittsburgh PA, 2003).^{36,37} Prior to docking studies, structures were checked in AutoDockTools 1.5.4 (The Scripps Research Institute, La Jolla, CA) for possible bond torsion errors, and appropriate Gasteiger charges were calculated and assigned as necessary. The crystal structure of

EGFR (L858R/T790M mutant) from the Brookhaven Protein Data Bank (PDB ID: 2JIV) was used as the receptor for docking studies, and the active site coordination ranges were defined using the grid box in AutoDockTools. The inhibitor structures were then docked into the active site using AutoDock Vina.³⁸ Conformational searches were performed with an exhaustiveness setting of '9'. Results were evaluated based on relative docking energies.

Synthesis of *N*-(3-Chloro-4-fluorophenyl)-7-ethoxy-6-nitroquinazolin-4-amine (2). A mixture of **1** (4.55 g, 18.0 mmol) in 40 mL of dichloromethane (DCM) and 3-chloro-4-fluoroaniline (2.61 g, 18.0 mmol) in 80 mL of isopropanol was stirred at room temperature overnight. The solid was collected and washed with a small amount of DCM to give 6.67 g (93%) of **2** as a bright yellow powder. ¹H NMR (300 MHz, DMSO-*d*₆) δ 11.69 (bs, 1H), 9.59 (s, 1H), 8.93 (s, 1H), 8.07 (dd, *J* = 6.8, 2.6 Hz, 1H), 7.77 (ddd, *J* = 9.0, 4.4, 2.6 Hz, 1H), 7.63 (s, 1H), 7.54 (t, *J* = 9.1 Hz, 1H), 7.27 (q, *J* = 8.8 Hz, 1H), 4.39 (q, *J* = 6.9 Hz, 2H), 1.44 (t, *J* = 6.9 Hz, 3H); ¹³C NMR (126 MHz, DMSO-*d*₆) δ 159.45, 156.29, 155.51, 154.99, 154.34, 139.92, 134.79, 126.18, 124.92, 123.34, 119.75, 117.54, 107.29, 105.92, 99.98, 66.76, 14.50; MS (ES) *m/z* 363.1 [M + H]⁺.

Synthesis of *N*⁴-(3-Chloro-4-fluorophenyl)-7-ethoxyquinazoline-4,6-diamine (3). A mixture of **2** (2 g, 5 mmol), iron (1.68 g, 30.1 mmol), acetic acid (1.8 g, 30.1 mmol), and sodium acetate (0.41 g, 5.0 mmol) in 80 mL of methanol was refluxed for 3 h. To this mixture were added 3 mL of conc. ammonia. The mixture was filtered while hot, the solid was washed with hot methanol, and the solvent was removed from the filtrate by rotary evaporation. The resulting solid was extracted four times with hot acetone. After the acetone was removed from the extracts, water was added to the residue, and the slurry was stirred for 30 min. The yellow precipitate was filtered, washed with water, and dried in a vacuum at 60 °C to yield 1.42 g (85%) of **3**. ¹H NMR (300 MHz, DMSO-*d*₆) δ 9.38 (s, 1H), 8.38 (s, 1H), 8.25–8.11 (m, 1H), 7.90–7.73 (m, 1H), 7.38 (m, 2H), 7.08 (s, 1H), 5.33 (s, 2H), 4.22 (q, *J* = 7.2 Hz, 2H), 1.45 (t, *J* = 7.0 Hz, 3H); ¹³C NMR (126 MHz, DMSO-*d*₆) δ 154.90, 153.51, 151.83, 151.58, 150.12, 144.70, 138.42, 137.46, 122.34, 121.34, 118.58, 116.38, 110.19, 106.24, 100.75, 63.77, 14.34; MS (ES) *m/z* 333.1 [M + H]⁺.

Synthesis of 1-(4-((3-Chloro-4-fluorophenyl)amino)-7-ethoxyquinazolin-6-yl)-3-methylthiourea (4). A mixture of 0.1 g (0.3 mmol) of **3** and 0.033 g (0.45 mmol) of methylisothiocyanate was stirred in 3 mL of ethanol at room temperature for 3 h. The solution was concentrated to half its volume and stored in the refrigerator overnight. The precipitate formed was collected, washed with ethanol to yield 47 mg (39%) of **4**. ¹H NMR (500 MHz, DMSO-*d*₆) δ 9.71 (s, 1H), 9.08 (s, 1H), 8.61 (s, 1H), 8.57 (s, 1H), 8.20 (dd, *J* = 6.8, 2.6 Hz, 1H), 7.84 (ddd, *J* = 9.2, 4.3, 2.7 Hz, 2H), 7.43 (t, *J* = 9.1 Hz, 1H), 7.26 (s, 1H), 4.24 (q, *J* = 7.0 Hz, 2H), 2.94 (d, *J* = 4.3 Hz, 3H), 1.41 (t, *J* = 6.9 Hz, 3H); ¹³C NMR (126 MHz, DMSO-*d*₆) δ 182.39, 157.41, 157.17, 154.69, 154.52, 152.59, 150.42, 137.22, 128.17, 123.57, 122.48, 121.31, 119.26, 117.07, 109.16, 108.22, 64.79, 31.94, 14.83; MS (ES) *m/z* 406.1 [M + H]⁺.

Synthesis of 1-(4-((3-Chloro-4-fluorophenyl)amino)-7-ethoxyquinazolin-6-yl)-3-phenylthiourea (5). This analogue was synthesized using the same procedure and stoichiometric amounts described for compound **4**. Yield 35 mg (25%). ¹H NMR (300 MHz, DMSO-*d*₆) δ 9.95 (s, 1H), 9.74 (s, 1H), 9.36 (s, 1H), 8.72 (s, 1H), 8.57 (s, 1H), 8.19 (dd, *J* = 6.9, 2.7 Hz, 1H), 7.83 (ddd, *J* = 9.4, 4.4, 2.7 Hz, 1H), 7.56–7.30 (m, 5H), 7.27 (s, 1H), 7.16 (t, *J* = 7.3 Hz, 1H), 4.26 (q, *J* = 6.9 Hz, 2H), 1.43 (t, *J* = 6.8 Hz, 3H); ¹³C NMR (126 MHz, DMSO-*d*₆) δ 180.38, 156.97, 156.69, 154.19, 154.17, 153.99, 152.06, 149.99, 139.17, 136.66, 128.41, 128.06, 124.72, 124.06, 123.12, 122.01, 121.16, 118.70, 116.50, 108.48, 107.54, 64.31, 14.32; MS (ES) *m/z* 468.2 [M + H]⁺.

Synthesis of *N*⁴-(3-Chloro-4-fluorophenyl)-7-ethoxy-*N*⁶-methylquinazoline-4,6-diamine (6). To a solution of sodium methoxide in 30 mL of methanol (prepared from 0.35 g/15 mmol of sodium metal) were added 1 g (3 mmol) of **3** and 0.45 g (15 mmol) of paraformaldehyde. The reaction mixture was refluxed for 2 h and subsequently cooled to 0 °C. After 0.57 g (15 mmol) of sodium tetrahydroborate were added in small portions, the orange mixture

turned light yellow, and heating at reflux was continued for another 2 h. Solvent was removed by rotary evaporation, and the residue was washed with water. The solid was then dissolved in a minimum amount of methanol/DCM (1:1), and the solution was passed through a Celite pad to remove a minor amount of a black solid. Solvent was removed to give 0.7 g (67%) of **6** as a light yellow powder. ¹H NMR (300 MHz, DMSO-*d*₆) δ 9.31 (s, 1H), 8.37 (s, 1H), 8.16 (dd, *J* = 6.9, 2.7 Hz, 1H), 7.84 (ddd, *J* = 9.1, 4.4, 2.6 Hz, 1H), 7.42 (t, *J* = 9.1 Hz, 1H), 7.13 (s, 1H), 7.05 (s, 1H), 5.71 (q, *J* = 5.1 Hz, 1H), 4.23 (q, *J* = 6.9 Hz, 2H), 2.92 (d, *J* = 4.9 Hz, 3H), 1.45 (t, *J* = 6.9 Hz, 3H); ¹³C NMR (75 MHz, DMSO-*d*₆) δ 154.77, 154.31, 151.69, 151.10, 149.94, 144.41, 139.89, 137.29, 122.83, 121.79, 118.67, 116.42, 110.15, 105.56, 95.67, 63.86, 30.03, 14.33; MS (ES) *m/z* 347.1 [M + H]⁺.

Synthesis of 1-(4-((3-Chloro-4-fluorophenyl)amino)-7-ethoxyquinazolin-6-yl)-1,3-dimethylthiourea (7). A mixture of 2.5 g (7.2 mmol) of **6**, 1.05 g (14.4 mmol) of methylisothiocyanate, and 1.76 g (14.4 mmol) of 4-dimethylaminopyridine (DMAP) in 20 mL of ethanol was stirred at reflux for 30 h. Additional methylisothiocyanate was added after 6, 18, and 24 h (2 equiv each time). Ethanol was removed and the resulting dark oil was applied to a triethylamine-treated silica gel column. DCM/methanol (50:1) was used to remove nonpolar impurities, and the same solvent at a 30:1 ratio was used to elute the product. The product fractions were combined, and solvent was removed by rotary evaporation. The residue was recrystallized from ethyl acetate to give 1.05 g (35%) of **7** as orange crystalline solid; ¹H NMR (500 MHz, DMSO-*d*₆) δ 9.72 (s, 1H), 8.61 (s, 1H), 8.48 (s, 1H), 8.23 (dd, *J* = 6.9, 2.7 Hz, 1H), 7.85 (ddd, *J* = 9.2, 4.3, 2.7 Hz, 1H), 7.44 (t, *J* = 9.1 Hz, 1H), 7.33 (s, 1H), 7.18 (s, 1H), 4.24 (q, *J* = 6.9 Hz, 2H), 3.47 (s, 3H), 2.85 (d, *J* = 4.2 Hz, 3H), 1.36 (t, *J* = 6.9 Hz, 3H); ¹³C NMR (126 MHz, DMSO-*d*₆) δ 183.41, 158.43, 157.37, 155.44, 154.59, 152.66, 151.97, 137.07, 133.10, 124.53, 123.48, 122.35, 119.33, 117.13, 109.82, 109.68, 64.81, 56.49, 19.02, 14.81; HRMS *m/z* [M + H]⁺ calcd for C₁₉H₂₀ClFN₅OS: 420.1061, found: 420.1032.

Synthesis of *N*⁴-(3-Chloro-4-fluorophenyl)-7-ethoxy-*N*⁶-(2-(methylamino)ethyl)quinazoline-4,6-diamine (8). A mixture containing 2.0 g (6.0 mmol) of **3**, 0.68 g (18 mmol) of NaCNBH₃, and 2.1 g (12 mmol) of *tert*-butylmethyl(2-oxoethyl)carbamate in 40 mL of methanol was prepared. Sufficient glacial acetic acid (~1.5 g) was added until the solid was completely dissolved. A yellow precipitate formed after the reaction was stirred for 12 h at room temperature. Solvent was removed and the resulting oil was redissolved in DCM, washed with saturated NaHCO₃ and brine, and dried over Na₂SO₄. DCM was removed and the residue was heated at reflux in 50 mL of 4 M HCl for 2 h to remove the Boc protecting group. Acid was removed by rotary evaporation, and the resulting oil was allowed to solidify by stirring in ethanol at room temperature overnight. The solid was collected, washed with small amounts of ethanol, and partitioned between DCM and 1 M NaOH solution. The organic layer was recovered, washed with brine, and dried over Na₂SO₄. After the solvent was removed 1.0 g (51%) of **8** was obtained as a white solid. ¹H NMR (300 MHz, DMSO-*d*₆) δ 9.31 (s, 1H), 8.37 (s, 1H), 8.15 (dd, *J* = 6.9, 2.6 Hz, 1H), 7.83 (ddd, *J* = 9.1, 4.4, 2.7 Hz, 1H), 7.42 (t, *J* = 9.1 Hz, 1H), 7.24 (s, 1H), 7.07 (s, 1H), 5.45 (t, *J* = 5.4 Hz, 1H), 4.24 (q, *J* = 6.9 Hz, 2H), 3.32 (q, *J* = 5.8 Hz, 2H), 2.84 (t, *J* = 6.0 Hz, 2H), 2.35 (s, 3H), 1.44 (t, *J* = 6.9 Hz, 3H); ¹³C NMR (126 MHz, DMSO-*d*₆) δ 154.82, 153.70, 151.77, 151.56, 150.16, 144.52, 138.77, 137.20, 122.93, 121.87, 118.63, 116.38, 110.04, 105.82, 96.42, 63.93, 49.75, 42.19, 35.81, 14.31; MS (ES) *m/z* 390.2 [M + H]⁺.

Synthesis of 1-(2-((4-((3-Chloro-4-fluorophenyl)amino)-7-ethoxyquinazolin-6-yl)amino)ethyl)-1,3-dimethylthiourea (9). A mixture of 0.14 g (1.92 mmol) of methylisothiocyanate and 0.5 g (1.28 mmol) of **8** in 10 mL of ethanol was stirred at room temperature for 1 h to produce a white solid precipitate, which was collected, washed with cold ethanol, and dried to yield 0.53 g (90%) of **9**. ¹H NMR (500 MHz, DMSO-*d*₆) δ 9.24 (s, 1H), 8.39 (s, 1H), 8.18 (dd, *J* = 6.9, 2.7 Hz, 1H), 7.85 (ddd, *J* = 9.1, 4.0, 2.7 Hz, 1H), 7.51 (q, *J* = 4.2 Hz, 1H), 7.43 (t, *J* = 9.1 Hz, 1H), 7.25 (s, 1H), 7.06 (s, 1H), 5.85 (t, *J* = 5.3 Hz, 1H), 4.22 (q, 2H), 4.16 (t, *J* = 6.4 Hz, 2H), 3.47 (q, *J* = 6.0 Hz, 2H), 3.10 (s, 3H), 2.94 (d, *J* = 4.1 Hz, 3H), 1.45 (t, *J* = 6.9 Hz, 3H); ¹³C NMR (126 MHz, DMSO-*d*₆) δ 182.50, 155.32, 154.22, 152.29, 152.17,

150.70, 145.11, 139.13, 137.76, 123.26, 122.19, 119.22, 116.99, 110.57, 106.31, 96.57, 64.51, 51.89, 41.95, 37.90, 33.19, 14.97; HRMS m/z [M + H]⁺ calcd for C₂₁H₂₅ClF₆N₆O₅: 463.1483, found: 463.1464.

Synthesis of [Au(7)]₂Cl₂ (12a). A mixture of 0.10 g (0.24 mmol) of compound 7 and 76 mg (0.24 mmol) of chlorotetrahydrothiophenogold(I) (10a) in 5 mL of DCM and 1 mL of methanol and was stirred at room temperature for 30 min. When the solution was concentrated to a volume of ~1 mL, compound 12a precipitated as an off-white solid, which was collected, washed with DCM, and dried in a vacuum at 60 °C. Yield: 0.116 g (75%). ¹H NMR (500 MHz, DMSO-*d*₆) δ 9.77 (s, 1H), 8.89 (s, 1H), 8.63 (s, 1H), 8.54 (s, 1H), 8.23–8.15 (m, 1H), 7.86–7.78 (m, 1H), 7.46 (t, *J* = 9.1 Hz, 1H), 7.33 (s, 1H), 4.25 (s, 2H), 3.53 (s, 3H), 3.17 (s, 3H), 1.45–1.30 (m, 3H); ¹³C NMR (126 MHz, DMSO-*d*₆) δ 175.87, 157.60, 157.44, 155.79, 154.75, 152.81, 152.02, 136.88, 133.21, 124.09, 123.79, 122.59, 119.37, 117.19, 109.68, 65.09, 55.37, 34.21, 14.88; HRMS m/z [M]²⁺ calcd for C₃₈H₃₈Au₂Cl₂F₂N₁₀O₂S₂: 616.0648, found: 616.0611; anal. calcd for C₃₈H₃₈Au₂Cl₂F₂N₁₀O₂S₂·CH₂Cl₂: C 33.20, H 2.71, N 10.19, found: C 33.49, H 2.65, N 10.13. (The analogous thiocyanate salt 12b showed the same mass spectroscopic and NMR features.)

Synthesis of [Au(9)PET₃](NO₃) (13). To 0.153 g (0.34 mmol) of 9 in a mixture of 10 mL of THF and 5 mL of methanol 0.122 g (0.34 mmol) of chlorotriethylphosphinegold(I) was added. The mixture was stirred for 5 min, and 56 μL of a 1 g/mL aqueous solution of AgNO₃ were added to exchange chloride with nitrate counterions. Precipitated AgCl was filtered off and the filtrate was concentrated and added to 20 mL of diethyl ether. Compound 13 precipitates as a yellow solid, which was washed with diethyl ether and dried in a vacuum. Yield: 0.126 g (46%). ¹H NMR (500 MHz, DMSO-*d*₆) δ 9.32 (s, 1H), 8.41 (s, 1H), 8.27 (q, *J* = 4.2 Hz, 1H), 8.15 (dd, *J* = 6.8, 2.6 Hz, 1H), 7.83 (ddd, *J* = 9.1, 4.0, 2.7 Hz, 1H), 7.44 (td, *J* = 9.1, 0.8 Hz, 1H), 7.29 (s, 1H), 7.10 (s, 1H), 5.77 (t, *J* = 5.35 Hz, 1H), 4.24 (q, *J* = 6.9 Hz, 2H), 4.19 (t, *J* = 5.6 Hz, 2H), 3.57 (q, *J* = 6.1 Hz, 2H), 3.21 (s, 3H), 3.10 (d, *J* = 4.0 Hz, 3H), 1.89 (dq, *J* = 10.6, 7.6 Hz, 6H), 1.45 (t, *J* = 6.9 Hz, 3H), 1.05 (dt, *J* = 19.3, 7.7 Hz, 9H); ¹³C NMR (126 MHz, DMSO-*d*₆) δ 175.45, 154.87, 153.77, 151.84, 151.76, 150.27, 144.14, 138.31, 137.01, 122.84, 121.78, 118.70, 116.49, 109.91, 105.65, 96.57, 64.05, 52.18, 40.8, 33.57, 16.78, 14.37, 8.94, 8.83; HRMS m/z [M]⁺ calcd for C₂₇H₃₉AuClF₆N₆O₅PS: 777.1982, found: 777.1957; anal. calcd for C₂₇H₃₉AuClF₆N₆O₅PS: C 38.65, H 4.68, N 11.67, found: C 38.13, H 4.25, N 10.79.

Cell Proliferation Assay. The human nonsmall cell lung cancer cell lines, NCI-H460 (large cell) and NCI-H1975 (adenocarcinoma), were obtained from the American Type Culture Collection (Rockville, MD, USA). Both cell lines were cultured in RPMI-1640 media (HyClone) supplemented with 10% fetal bovine serum (FBS), 10% penstrep (P&S), 10% L-glutamine, and 1.5 g/L NaHCO₃. Cells were incubated at a constant temperature at 37 °C in a humidified atmosphere containing 5% CO₂ and were subcultured every 2–3 days in order to maintain cells in logarithmic growth. The cytotoxicity studies were carried out according to a standard protocol using the Celltiter 96 aqueous nonradioactive cell proliferation assay kit (Promega, Madison, WI). Stock solutions (10 mM) of all drugs were prepared in DMF and serially diluted with media to a final concentration of less than 0.1 μM prior to incubation with cancer cells. IC₅₀ values were calculated from dose–response curves using sigmoidal curve fits in GraphPad Prism, version 5.00 (GraphPad Software Inc., La Jolla, CA).

Enzyme Inhibition Assay. Compounds were tested against epidermal growth factor receptor tyrosine kinase, EGFR_{L858R/T790M} using the ADP-Glo Kinase assay platform (Promega, Madison, WI). Reactions were performed on white 96-well plates (BD Biosciences, San Jose, CA). Stock solutions (1 mM) were prepared in DMF, and serial dilutions were carried out in a modified 1× kinase reaction buffer, which was free of bovine serum albumin (BSA) and dithiothreitol (DTT) (40 mM Tris-HCl, pH 7.5; 20 mM MgCl₂; 2 mM MnCl₂; 0.05 mM Na₂S₂O₄). To estimate the amount of ADP generated by EGFR-TK and to determine the optimal amount of enzyme in assay reactions, standard curves of luminescence intensity vs

% ATP-to-ADP conversion for [ATP] up to 100 μM were plotted, which show the expected linearity over the entire concentration range (data not shown). Reactions contained 44 ng of EGFR in 10 μL of buffer, 10 μL of 250 μM ATP/0.2 μg/μL poly(Glu₄Tyr₁), and 5 μL of inhibitor in 1× reaction buffer (total volume 25 μL, final [ATP] = 100 μM). Mixtures were incubated for 60 min and subsequently terminated by adding 25 μL of ADP-Glo reagent (Promega). Termination reactions were allowed to incubate for 40 min, and 50 μL of kinase detection reagent (Promega) was added. The plates were then analyzed for luminescence with a Synergy H1 Hybrid Reader (BioTek, Winooski, VT) after 30 min of incubation. IC₅₀ values were calculated from sigmoidal curve fits of the luminescence data using GraphPad Prism from an average from two determinations.

■ ASSOCIATED CONTENT

Supporting Information

Molecular docking results, details for compound characterization and stability studies (NMR and electrospray mass spectra, solid state structure of compound 9), and results of the enzyme inhibition assay. This material is available free of charge via the Internet at <http://pubs.acs.org>.

■ AUTHOR INFORMATION

Corresponding Author

*E-mail: bierbau@wfu.edu. Fax: 336-758-4656. Ph: 336-758-3507.

Notes

The authors declare no competing financial interest.

■ ACKNOWLEDGMENTS

This work was supported by a grant from the Science Research Fund of Wake Forest University. X.Q. gratefully acknowledges support from the China Scholarship Council (Grant 2011694010). DFT calculations were performed on the Wake Forest University DEAC Cluster, a centrally managed resource with support provided in part by the University. The HRMS data were acquired on a Thermo Scientific LTQ Orbitrap instrument, which was purchased with funds provided by the NSF (Grant Award Number 947028).

■ REFERENCES

- (1) Berners-Price, S. J.; Filipovska, A. *Metalomics* **2011**, 3, 863–873.
- (2) Erdogan, E.; Lamark, T.; Stallings-Mann, M.; Lee, J.; Pellecchia, M.; Thompson, E. A.; Johansen, T.; Fields, A. P. *J. Biol. Chem.* **2006**, 281, 28450–28459.
- (3) Abbehausen, C.; Peterson, E. J.; de Paiva, R. E.; Corbi, P. P.; Formiga, A. L.; Qu, Y.; Farrell, N. P. *Inorg. Chem.* **2013**, 52, 11280–11287.
- (4) Fernandez-Gallardo, J.; Elie, B. T.; Sulzmaier, F. J.; Sanau, M.; Ramos, J. W.; Contel, M. *Organometallics* **2014**, 33, 6669–6681.
- (5) Yoshida, T.; Zhang, G.; Haura, E. B. *Biochem. Pharmacol.* **2010**, 80, 613–623.
- (6) Kumar, A.; Petri, E. T.; Halmos, B.; Boggon, T. J. *J. Clin. Oncol.* **2008**, 26, 1742–1751.
- (7) Paez, J. G.; Janne, P. A.; Lee, J. C.; Tracy, S.; Greulich, H.; Gabriel, S.; Herman, P.; Kaye, F. J.; Lindeman, N.; Boggon, T. J.; Naoki, K.; Sasaki, H.; Fujii, Y.; Eck, M. J.; Sellers, W. R.; Johnson, B. E.; Meyerson, M. *Science* **2004**, 304, 1497–1500.
- (8) Sharma, S. V.; Bell, D. W.; Settleman, J.; Haber, D. A. *Nat. Rev. Cancer* **2007**, 7, 169–181.
- (9) Pao, W.; Miller, V.; Zakowski, M.; Doherty, J.; Politi, K.; Sarkaria, I.; Singh, B.; Heelan, R.; Rusch, V.; Fulton, L.; Mardis, E.; Kupfer, D.; Wilson, R.; Kris, M.; Varmus, H. *Proc. Natl. Acad. Sci. U. S. A.* **2004**, 101, 13306–13311.

- (10) Yun, C. H.; Mengwasser, K. E.; Toms, A. V.; Woo, M. S.; Greulich, H.; Wong, K. K.; Meyerson, M.; Eck, M. J. *Proc. Natl. Acad. Sci. U. S. A.* **2008**, *105*, 2070–2075.
- (11) Liu, Q.; Sabnis, Y.; Zhao, Z.; Zhang, T.; Buhrlage, S. J.; Jones, L. H.; Gray, N. S. *Chem. Biol.* **2013**, *20*, 146–159.
- (12) Hirsh, V. *Future Oncol.* **2011**, *7*, 817–825.
- (13) Zhang, J.; Yang, P. L.; Gray, N. S. *Nat. Rev. Cancer* **2009**, *9*, 28–39.
- (14) Eiter, L. C.; Hall, N. W.; Day, C. S.; Saluta, G.; Kucera, G. L.; Bierbach, U. *J. Med. Chem.* **2009**, *52*, 6519–6522.
- (15) Yan, K.; Lok, C. N.; Bierla, K.; Che, C. M. *Chem. Commun.* **2010**, *46*, 7691–7693.
- (16) Ahmad, S.; Isab, A. A. *J. Inorg. Biochem.* **2002**, *88*, 44–52.
- (17) Cha, M. Y.; Lee, K. O.; Kim, J. W.; Lee, C. G.; Song, J. Y.; Kim, Y. H.; Lee, G. S.; Park, S. B.; Kim, M. S. *J. Med. Chem.* **2009**, *52*, 6880–6888.
- (18) Uson, R.; Laguna, A.; Laguna, M.; Briggs, D. A.; Murray, H. H.; Fackler, J. P. *Inorg. Synth.* **1989**, *26*, 85–91.
- (19) Levallet, C.; Lerpiniere, J.; Ko, S. Y. *Tetrahedron* **1997**, *53*, 5291–5304.
- (20) Mann, F. G.; Wells, A. F.; Purdie, D. *J. Chem. Soc.* **1937**, 1828.
- (21) Marcaurelle, L. A.; Comer, E.; Dandapani, S.; Duvall, J. R.; Gerard, B.; Kesavan, S.; Lee, M. D. t.; Liu, H.; Lowe, J. T.; Marie, J. C.; Mulrooney, C. A.; Pandya, B. A.; Rowley, A.; Ryba, T. D.; Suh, B. C.; Wei, J.; Young, D. W.; Akella, L. B.; Ross, N. T.; Zhang, Y. L.; Fass, D. M.; Reis, S. A.; Zhao, W. N.; Haggarty, S. J.; Palmer, M.; Foley, M. A. *J. Am. Chem. Soc.* **2010**, *132*, 16962–16976.
- (22) Hamed, M. M.; Abou El Ella, D. A.; Keeton, A. B.; Piazza, G. A.; Abadi, A. H.; Hartmann, R. W.; Engel, M. *ChemMedChem* **2013**, *8*, 1495–1504.
- (23) Gajiwala, K. S.; Feng, J.; Ferre, R.; Ryan, K.; Brodsky, O.; Weinrich, S.; Kath, J. C.; Stewart, A. *Structure* **2013**, *21*, 209–219.
- (24) Zhou, W.; Ercan, D.; Chen, L.; Yun, C. H.; Li, D.; Capelletti, M.; Cortot, A. B.; Chirieac, L.; Iacob, R. E.; Padera, R.; Engen, J. R.; Wong, K. K.; Eck, M. J.; Gray, N. S.; Janne, P. A. *Nature* **2009**, *462*, 1070–1074.
- (25) Li, D.; Ambrogio, L.; Shimamura, T.; Kubo, S.; Takahashi, M.; Chirieac, L. R.; Padera, R. F.; Shapiro, G. I.; Baum, A.; Himmelsbach, F.; Rettig, W. J.; Meyerson, M.; Solca, F.; Greulich, H.; Wong, K. K. *Oncogene* **2008**, *27*, 4702–4711.
- (26) Kouodom, M. N.; Ronconi, L.; Celegato, M.; Nardon, C.; Marchio, L.; Dou, Q. P.; Aldinucci, D.; Formaggio, F.; Fregona, D. *J. Med. Chem.* **2012**, *55*, 2212–2226.
- (27) Akerman, K. J.; Fagenson, A. M.; Cyril, V.; Taylor, M.; Muller, M. T.; Akerman, M. P.; Munro, O. Q. *J. Am. Chem. Soc.* **2014**, *136*, 5670–5682.
- (28) Meyer, A.; Oehninger, L.; Geldmacher, Y.; Alborzinia, H.; Wölfl, S.; Sheldrick, W. S.; Ott, I. *ChemMedChem* **2014**, *9*, 1794–800.
- (29) Koster, S. D.; Alborzinia, H.; Can, S. Z.; Kitanovic, I.; Wölfl, S.; Rubbiani, R.; Ott, I.; Riesterer, P.; Prokop, A.; Merz, K.; Metzler-Nolte, N. *Chem. Sci.* **2012**, *3*, 2062–2072.
- (30) Dempke, W. C.; Suto, T.; Reck, M. *Lung Cancer* **2010**, *67*, 257–274.
- (31) Meggers, E. *Chem. Commun.* **2009**, 1001–1010.
- (32) Isab, A. A.; Fettouhi, M.; Ahmad, S.; Ouahab, L. N. *Polyhedron* **2003**, *22*, 1349–1354.
- (33) Gandin, V.; Fernandes, A. P.; Rigobello, M. P.; Dani, B.; Sorrentino, F.; Tisato, F.; Bjornstedt, M.; Bindoli, A.; Sturaro, A.; Rella, R.; Marzano, C. *Biochem. Pharmacol.* **2010**, *79*, 90–101.
- (34) Sordella, R.; Bell, D. W.; Haber, D. A.; Settleman, J. *Science* **2004**, *305*, 1163–1167.
- (35) Deng, J.; Shimamura, T.; Perera, S.; Carlson, N. E.; Cai, D.; Shapiro, G. I.; Wong, K. K.; Letai, A. *Cancer Res.* **2007**, *67*, 11867–11875.
- (36) Frisch, M. J.; Trucks, G. W.; Schlegel, H. B.; Scuseria, G. E.; Robb, M. A.; Cheeseman, J. R.; Montgomery, J. A.; Vreven, T.; Kudin, K. N.; Burant, J. C.; Millam, J. M.; Iyengar, S. S.; Tomasi, J.; Barone, V.; Mennucci, B.; Cossi, M.; Scalmani, G.; Rega, N.; Petersson, G. A.; Nakatsuji, H.; Hada, M.; Ehara, M.; Toyota, K.; Fukuda, R.; Hasegawa, J.; Ishida, M.; Nakajima, T.; Honda, Y.; Kitao, O.; Nakai, H.; Klene, M.; Li, X.; Knox, J. E.; Hratchian, H. P.; Cross, J. B.; Bakken, V.; Adamo, C.; Jaramillo, J.; Gomperts, R.; Stratmann, R. E.; Yazyev, O.; Austin, A. J.; Cammi, R.; Pomelli, C.; Ochterski, J. W.; Ayala, P. Y.; Morokuma, K.; Voth, G. A.; Salvador, P.; Dannenberg, J. J.; Zakrzewski, V. G.; Dapprich, S.; Daniels, A. D.; Strain, M. C.; Farkas, O.; Malick, D. K.; Rabuck, A. D.; Raghavachari, K.; Foresman, J. B.; Ortiz, J. V.; Cui, Q.; Baboul, A. G.; Clifford, S.; Cioslowski, J.; Stefanov, B. B.; Liu, G.; Liashenko, A.; Piskorz, P.; Komaromi, I.; Martin, R. L.; Fox, D. J.; Keith, T.; Laham, A.; Peng, C. Y.; Nanayakkara, A.; Challacombe, M.; Gill, P. M. W.; Johnson, B.; Chen, W.; Wong, M. W.; Gonzalez, C.; Pople, J. A. *Gaussian 03*, Revision D.02; Gaussian Inc.: Wallingford, CT, 2003.
- (37) Dunning, T. H. J.; Hay, P. J. *Mod. Theor. Chem.* **1977**, *3*, 1–27.
- (38) Trott, O.; Olson, A. J. *J. Comput. Chem.* **2010**, *31*, 455–461.